Supporting Information

Negative hyperconjugation effect on the reactivity of phosphoramide mustard derivatives as a DNA alkylating agent: theoretical and experimental insights

Mahyar Bonsaii, Khodayar Gholivand,* Morteza Khosravi and Khosrou Abdi

Molecular modeling and docking

The crystal structures of the DNA–ligand complex were selected from the PDB (ID 2B1D).[1] This crystal structure was prepared using the Protein Preparation Wizard in Schrödinger's Maestro suite (version 11, Schrödinger, LLC, New York, NY, 2016). All water molecules and other groups (except for the ligand) were removed. Preprocessing was carried out with "Assign bond orders", "Add hydrogens" and "Fill in missing side chains using Prime" options. For H-bond assignment in the refinement step, "Exhaustive sampling" and "Sample at pH Neutral" were selected. Final structure minimization was performed with default settings using the OPLS-3 force field.[2–4] All studied ligand molecules were sketched and cleaned using the builder tools option implemented in the Maestro. The molecules were then optimized with the Jaguar (B3LYP/6-31**) and the LigPrep utility (pH 7.4).

The resulting structures of DNA and ligand molecules were used for docking in Glide (version 7.1, Schrödinger, LLC, New York, NY, 2016.).[5–6] For every individual model, the correlation between calculated binding and experimental values was analyzed to determine the most representative item. Glide requires prepared receptor grids for docking. Grid size was assigned automatically and focalized at the centroid of the reference ligand from the crystallographic structure. Docking to the macromolecule was carried out using the extra precision (XP) mode. The Glide XP scoring, which is a modified version of the Chemscore, [7] was used to assess the binding of small molecules to DNA. The XP scoring function contains four main components that accounts for: i) Coulomb energy of the interacting atoms (E_{coul}), ii) the van der Waal's energy of atoms (E_{vdW}), iii) a collection of terms that favor binding interactions (E_{bind}), and iv) a collection of terms that hinder binding interactions ($E_{penalty}$).[8]

$$XP\ GlideScore = E_{coul} + E_{vdW} + E_{bind} + E_{penalty} \quad (1)$$

$$E_{bind} = E_{hyd\_enclosure} + E_{hb\_nn\_motif} + E_{hb\_cc\_motif} + E_{PI} + E_{hb\_pair} + E_{phobic\_pair} \quad (2)$$

$$E_{penalty} = E_{desolv} + E_{ligand\_strain} \quad (3)$$

In equations (2) and (3), $E_{hyd\_enclosure}$ is the hydrophobic enclosure reward, $E_{hb\_nn\_motif}$ is the term for neutral-neutral hydrogen bonds in a hydrophobically enclosed environment, $E_{hb\_cc\_motif}$ is the term for special charged-charged hydrogen bonds, E_{PI} is the π-stacking/π-cation reward, E_{hb_pair} is the Chemscore-like pair hydrogen-bond term, E_{phobic_pair} is the pair lipophilic term, E_{desolv} is the water desolvation energy term and E_{ligand_strain} is the strain energy term.[5]

Apropos of nitrogen mustards interaction with DNA (N7 of guanine), Covalent Docking algorithm (CovDock) was used.[9–11]

To convert between the binding constant, $K_{binding}$, and the binding free energy change of binding, $\Delta G_{binding}$, we used the following equation:

$$\Delta G_{binding} = -RT\ lnK_{binding} \quad (4)$$

where R is the gas constant, 1.987 cal K^{-1} mol^{-1} and T is the absolute temperature, assumed to be room temperature, 298.15 K.

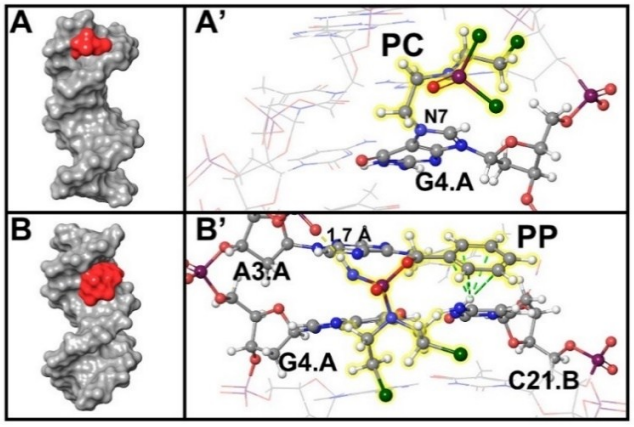

Fig. S1 Surface representation of d(GCAGACGTCTGC)$_2$ complexes with PC (A) and PP (B). Docking structure between d(GCAGACGTCTGC)$_2$ (PDB ID 2B1D) and PC (A'), PP (B').

The docking results are shown in Fig. S1. The PC docking (covalent docking) data show minor groove binding to oligonucleotide (2B1D), with a change in the angle of G–C (Fig. S1A and A') and binding free energy = –6.55 kcal mol^{-1}. These results are entirely consistent with IR data, conformational changes in DNA and experimental binding free energy (–7.48 kcal mol^{-1}). The models show that PP (Fig. S1B and B') is surrounded by G4.A, C21.B and a phosphate group of A3.A through hydrogen bonding in the major groove with binding free energy= –4.62 kcal mol^{-1}. This value is comparable with the experimental value (–5.1 kcal mol^{-1}).

Drug activation

The structures of the nitrogen mustards and their respective aziridinium ions are shown in Scheme 2, and Fig. S2 compares the computed reaction energy profiles of CPa, PMa, PCa and PPa. The transition state energy differences between the PM and other mustards are much greater than anticipated: phosphoramide mustard (PMa) forms the associated aziridinium ion PMb traversing at 19.06 kcal mol^{-1} in water, whereas the same reaction requires an activation barrier of 44.73 kcal mol^{-1} in the case of cyclophosphamide (CPa). The transition state associated with the model compound PPa is found at 62.70 kcal mol^{-1}, indicating that the Benzyl moiety in PPa has a high impact on the reaction profile.

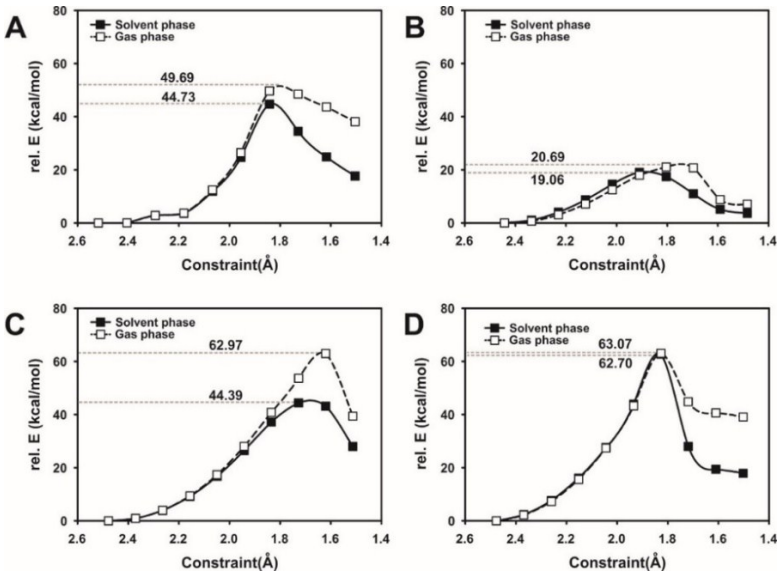

Fig. S2 Computed reaction profile for the formation of aziridinium ion from CP (A), PM (B), PC (C), and PP (D) in solvent (water) and gas phase (B3LYP/6-311**++).

Natural resonance theory (NRT) structures

The results of NRT resonance structures mentioned in the article are summarized in Figure S3.

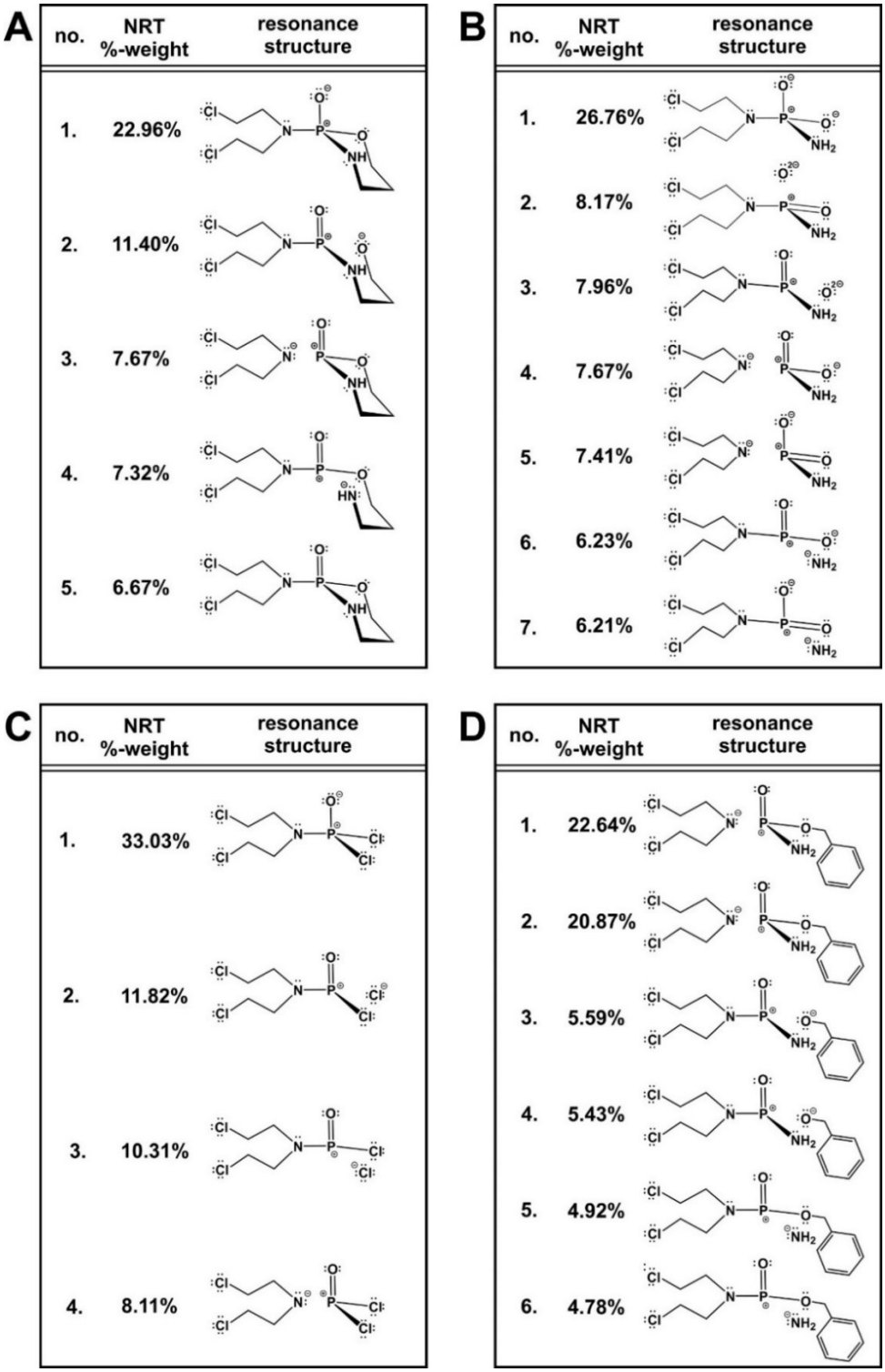

Fig. S3 NRT resonance structures of CP (A), PM (B), PC (C), and PP (D) beside Weightings.

Molecular orbital energy

Table S1 presents the energies of the frontier molecular orbitals for nitrogen mustards, computed in four different functional methods. Results show slight variations between 6-311g**++ and cc-pvtz(-f)++ basis sets in one of the procedures. Although the values of M06-2X are less than B3LYP, the process of variation is the same. Because of the widespread use of B3LYP/6-311g**++ in chemistry in this paper, the values were expressed in terms comparabile with that.

Table S1 Molecular orbital energies (in eV) of the HOMOs and LUMOs for nitrogen mustard active forms (CPa–PPc)

	B3LYP/6-311g**++		B3LYP/cc-pvtz(-f)++		M06-2X/6-311g**++		M06-2X/cc-pvtz(-f)++	
Compound	HOMO(eV)	LUMO(eV)	HOMO(eV)	LUMO(eV)	HOMO(eV)	LUMO(eV)	HOMO(eV)	LUMO(eV)
CPa	–7.12	–0.73	–7.08	–0.77	–8.73	–0.50	–8.69	–0.56
CPb	–11.36	–3.99	–11.36	–3.95	–13.01	–3.46	–13.01	–3.44
CPc	–10.11	–5.99	–10.06	–5.94	–11.72	–5.14	–11.67	–5.06
PMa	–2.47	2.44	–2.43	2.25	–4.06	2.55	–4.04	2.28
PMb	–7.69	–0.68	–7.69	–0.68	–7.69	–0.68	–7.69	–0.68
PMc	–10.58	–6.16	–10.53	–6.11	–12.15	–5.27	–12.11	–5.19
CPa	–8.08	–2.08	–7.97	–1.95	–9.63	–0.93	–9.49	–0.84
CPb	–11.86	–6.64	–11.82	–6.52	–13.51	–5.45	–13.45	–5.32
CPc	–11.07	–6.65	–11.02	–6.58	–12.69	–5.75	–12.63	–5.64
PPa	–7.19	–1.07	–7.14	–1.06	–8.64	–0.41	–8.62	–0.45
PPb	–10.30	–4.27	–10.27	–4.23	–11.65	–3.38	–11.62	–3.35
PPc	–9.75	–6.13	–9.73	–6.09	–11.09	–5.26	–11.06	–5.20

References

1 J. W. Locasale, A. A. Napoli, S. Chen, H. M. Berman and C. L. Lawson, *J. Mol. Biol*., 2009, **386**, 1054–1065.

2 T. Frączek, A. Siwek and P. Paneth, *J. Chem. Inf. Model*., 2013, **53**, 3326–3342.

3 D. Shivakumar, J. Williams, Y. Wu, W. Damm, J. Shelley and W. Sherman, *J. Chem. Theory Comput*., 2010, **6**, 1509–1519.

4 E. Harder, W. Damm, J. Maple, C. Wu, M. Reboul, J. Y. Xiang, L. Wang, D. Lupyan, M. K. Dahlgren, J. L. Knight, J. W. Kaus, D. S. Cerutti, G. Krilov, W. L. Jorgensen, R. Abel and R. A. Friesner, *J. Chem. Theory Comput*., 2016, **12**, 281–296.

5 R. A. Friesner, R. B. Murphy, M. P. Repasky, L. L. Frye, J. R. Greenwood, T. A. Halgren, P. C. Sanschagrin and D. T. Mainz, *J. Med. Chem*., 2006, **49**, 6177–6196.

6 T. A. Halgren, R. B. Murphy, R. A. Friesner, H. S. Beard, L. L. Frye, W. T. Pollard and J. L. Banks, *J. Med. Chem*., 2004, **47**, 1750–1759.

7 M. D. Eldridge, C. W. Murray, T. R. Auton, G. V. Paolini and R. P. Mee, *J. Comput.-Aided Mol. Des*., 1997, **11**, 425–445.

8 U. Yadava, H. Gupta, R. K. Yadav and M. Roychoudhury, *Adv. Sci. Lett*., 2014, **20**, 1637–1643.

9 K. Zhu, K. W. Borrelli, J. R. Greenwood, T. Day, R. Abel, R. S. Farid and E. Harder, *J. Chem. Inf. Model*., 2014, **54**, 1932–1940.

10 D. Toledo Warshaviak, G. Golan, K. W. Borrelli, K. Zhu and O. Kalid, *J. Chem. Inf. Model*., 2014, **54**, 1941–1950.

11 C. Scholz, S. Knorr, K. Hamacher and B. Schmidt, *J. Chem. Inf. Model*., 2015, **55**, 398–406.